



Elevated Expression of MiR-17 in Microglia of Alzheimer's Disease Patients Abrogates Autophagy-Mediated Amyloid- β Degradation

OPEN ACCESS

Edited by:

Maya Koronyo-Hamaoui,
Cedars Sinai Medical Center,
United States

Reviewed by:

Igal Ifergan,
University of Cincinnati,
United States
Ana Lloret,
University of Valencia, Spain

*Correspondence:

Amal O. Amer
amal.amer@osumc.edu

[†]These authors have contributed
equally to this work and share
first authorship

Specialty section:

This article was submitted to
Multiple Sclerosis
and Neuroimmunology,
a section of the journal
Frontiers in Immunology

Received: 05 May 2021

Accepted: 30 June 2021

Published: 27 July 2021

Citation:

Estfanous S, Daily KP, Eltobgy M,
Deems NP, Anne MNK, Krause K,
Badr A, Hamilton K, Carafice C,
Hegazi A, Abu Khweek A, Kelani H,
Nimjee S, Awad H, Zhang X, Cormet-
Boyaka E, Hafez H, Soror S, Mikhail A,
Nuovo G, Barrientos RM, Gavrilin MA
and Amer AO (2021) Elevated
Expression of MiR-17 in Microglia
of Alzheimer's Disease Patients
Abrogates Autophagy-Mediated
Amyloid- β Degradation.
Front. Immunol. 12:705581.
doi: 10.3389/fimmu.2021.705581

Shady Estfanous^{1,2†}, Kylene P. Daily^{1†}, Mostafa Eltobgy^{1†}, Nicholas P. Deems³,
Midhun N. K. Anne¹, Kathrin Krause^{1,4}, Asmaa Badr¹, Kaitlin Hamilton¹, Cierra Carafice¹,
Ahmad Hegazi¹, Arwa Abu Khweek^{1,5}, Hesham Kelani⁶, Shahid Nimjee⁷, Hamdy Awad⁶,
Xiaoli Zhang⁸, Estelle Cormet-Boyaka⁹, Hesham Hafez^{2,10}, Sameh Soror^{2,10}, Adel Mikhail¹¹,
Gerard Nuovo¹¹, Ruth M. Barrientos³, Mikhail A. Gavrilin¹² and Amal O. Amer^{1*}

¹ Department of Microbial Infection and Immunity, Infectious Diseases Institute, The Heart and Lung Research Institute, Ohio State University, Columbus, OH, United States, ² Biochemistry and Molecular Biology Department, Faculty of Pharmacy, Helwan University, Cairo, Egypt, ³ Institute for Behavioral Medicine Research, Ohio State University, Columbus, OH, United States, ⁴ Max Planck Unit for the Science of Pathogens, Berlin, Germany, ⁵ Department of Biology and Biochemistry, Birzeit University, West Bank, Palestine, ⁶ Department of Anesthesiology, Wexner Medical Center, The Ohio State University, Columbus, OH, United States, ⁷ Department of Neurological Surgery, Wexner Medical Center, The Ohio State University, Columbus, OH, United States, ⁸ Center for Biostatistics, Ohio State University, Columbus, OH, United States, ⁹ Department of Veterinary Biosciences, The Ohio State University, Columbus, OH, United States, ¹⁰ Center of Excellence, Helwan Structure Biology Research, Cairo, Egypt, ¹¹ GNOME DIAGNOSTICS, Department of Scientific Research, Powell, OH, United States, ¹² Department of Internal Medicine, Ohio State University, Columbus, OH, United States

Autophagy is a proposed route of amyloid- β (A β) clearance by microglia that is halted in Alzheimer's Disease (AD), though mechanisms underlying this dysfunction remain elusive. Here, primary microglia from adult AD (5xFAD) mice were utilized to demonstrate that 5xFAD microglia fail to degrade A β and express low levels of autophagy cargo receptor NBR1. In 5xFAD mouse brains, we show for the first time that AD microglia express elevated levels of microRNA cluster Mirc1/Mir17-92a, which is known to downregulate autophagy proteins. By *in situ* hybridization in post-mortem AD human tissue sections, we observed that the Mirc1/Mir17-92a cluster member *miR-17* is also elevated in human AD microglia, specifically in the vicinity of A β deposits, compared to non-disease controls. We show that NBR1 expression is negatively correlated with expression of *miR-17* in human AD microglia via immunohistopathologic staining in human AD brain tissue sections. We demonstrate in healthy microglia that autophagy cargo receptor NBR1 is required for A β degradation. Inhibiting elevated *miR-17* in 5xFAD mouse microglia improves A β degradation, autophagy, and NBR1 puncta formation *in vitro* and improves NBR1 expression *in vivo*. These findings offer a mechanism behind dysfunctional autophagy in AD microglia which may be useful for therapeutic interventions aiming to improve autophagy function in AD.

Keywords: autophagy, microglia, NBR1, microRNA, Amyloid- β , Alzheimer's disease, Mir17-92a

INTRODUCTION

Alzheimer's disease (AD) is the most common form of dementia worldwide and is characterized by chronic and irreversible neuronal degradation downstream of complex pathophysiological processes (1). One hallmark of AD is the presence of plaques primarily composed of insoluble amyloid- β (A β). A β accumulates in AD in a variety of forms, including soluble, oligomeric and fibrillar (2). The rate of A β clearance in healthy individuals is comparable to the rate of production (3). Accumulation of A β in the brain is a predisposing factor contributing to AD pathobiology usually preceding Tau tangle pathology (4). This strongly suggests that improving A β clearance is needed at early stages of the disease. To do so, a better understanding of the underlying defect is urgently required.

Microglia, brain resident immune cells, maintain tissue homeostasis by phagocytosis of dead cells, debris and toxic material such as extracellular A β (5). Microglia can participate in A β clearance by releasing enzymes that degrade A β in the extracellular space or by phagocytosing A β and degrading A β intracellularly within lysosomal compartments (6–8). Despite the capacity of healthy microglia to clear different forms of A β , reports suggest that AD microglia do not efficiently perform this function throughout AD (8–10). One proposed mechanism of A β degradation by microglia after internalization is autophagy (11–13). Autophagy is a conserved homeostatic cellular process for the degradation of extracellular and intracellular materials (14). Typically, extracellular materials destined for autophagy are phagocytosed by immune cells and marked by “eat me” signals, including poly-ubiquitin (14). Then, autophagy receptors such as p62/SQSTM1, NDP52, OPTN (optineurin), or NBR1 (neighbor of BRCA1 gene 1) bind to the ubiquitinated cargo and recruit LC3, bringing the nascent autophagosome (14, 15). Cargo-carrying autophagosomes mature and fuse with lysosomes where degradation of the autophago-lysosome-enclosed material occurs (14). The implication of dysfunctional autophagy in AD pathogenesis and A β degradation have been investigated but studies mainly focused on neuronal cells (16, 17). Few studies have shown that dysfunctional autophagy has significant consequences in AD microglia, including failure to regulate harmful neuroinflammation (17, 18). Emerging reports described a role for autophagy-mediated degradation of A β in AD, yet these studies were performed in cell lines or neonatal microglia, but not in diseased adult AD microglia and underlying mechanisms for dysfunctional autophagy in AD were not offered (11–13). Prolonged exposure to A β has been shown to disrupt autophagy in microglia, however, underlying cellular changes in response to A β leading to this disruption also remain unknown (19).

MicroRNAs (*MiRs*) are implicated in autophagy regulation (20) and AD progression (21), though there is no evidence of *MiRs* regulating autophagy in AD microglia. *MiRs* are evolutionarily conserved noncoding RNAs which mediate post-transcriptional gene silencing by binding to the 3'-untranslated region (UTR) or open reading frame (ORF) region of target mRNAs (22). Considering the strong implication of *MiRs* in both AD pathogenesis (21, 23) and autophagy function (20) and given

the lack of evidence linking these two fundamental processes, we searched for *MiRs* that regulate autophagy whose expression is altered in AD. Members of the *Mirc1/Mir17-92* *MiR* cluster are known to target essential autophagy molecules (24). Diminished expression of an individual autophagy protein targeted by elevated *MiRs* can halt autophagic function which will not be recovered by expression of other autophagy proteins (24). The *Mirc1/Mir17-92* cluster, represented by *miR-17-5p*, *miR-18a*, *miR-19a*, *miR-20a*, *miR-19b-1*, and *miR-92a-1*, is conserved among vertebrates and associated with roles in cell cycle, tumorigenesis, and aging (25).

In this study we investigate the role of the *Mirc1/Mir17-92* cluster in AD. We find that expression of the cluster increases specifically in microglia of AD mouse model (5x*FAD*) mice as they age. This upregulation is more prominent in the brains of AD human patients, when comparing with non-AD age- and sex-matched counterparts. Notably, expression of *miR-17-5p* (*miR-17*) is elevated in microglia adjacent to A β deposits but not in microglia away from deposits in the same human brain tissue sample. In addition, increased expression of *miR-17* correlates with reduced expression of target autophagy cargo receptor NBR1, which we demonstrate is needed for efficient A β degradation. Further, elevation of cluster component *miR-17* is largely responsible for defective clearance of A β by AD microglia, as inhibiting *miR-17* alone improves degradation of A β , autophagy and NBR1 puncta formation *in vitro* and restores expression of NBR1 in microglia *in vivo*. Our study advances our understanding of the role of microglial autophagy in the clearance of A β and provides a mechanistic basis for dysfunctional autophagy in AD microglia in human and mice.

MATERIALS AND METHODS

Human Samples From NIH Biobank

Human temporal lobe brain tissue sections (Brodmann area 38) from patients with AD and age-matched controls without dementia were obtained from the NIH biobank in accordance with our institution's IRB. These snap-frozen tissue samples were used for all TRIzol homogenization, RT-qPCR and immunoblot analysis. Range of hours until freeze, age, and sex are in **Supplemental Table 1**. The presence of A β deposits within homogenized samples is shown in **Supplemental Figure 2B**. Equal number of samples (n=15) for AD and age- and sex-matched non-AD controls were analyzed in determining *MiR* expression (**Figure 5A**) and (n=10) total brain homogenate NBR1 and A β burden (**Supplementary Figure 2**). Results were similar when data analysis was segregated by sex (data not shown). AD (BRAAK III or IV) and age-matched control hippocampal tissue sections utilized for *in situ* hybridization (ISH) and immunohistochemical analysis were obtained from the Discovery Life Science (DLS) tissue bank by G. Nuovo (26). Analysis of NBR1 in different cell types was performed in 3 AD and 3 control samples (**Figure 3A**). Analysis of NBR1 in different AD brain regions was performed in A β -negative and A β -positive regions from 3 unique patient samples (**Figure 3C**). Analysis of *miR-17* and A β was performed in 4 AD and 4 control samples, or

A β -negative and A β -positive regions from 4 unique patient samples (**Figures 5B–E**). Analysis of NBR1 with either TMEM (microglia) or neurons (pyruvate dehydrogenase) was performed in 3 unique AD patients in A β -positive regions (**Figures 5F, G**). Correlation analyses of *miR-17* and NBR1 in **Figure 7** were performed on 4 patients for AD and 4 patients for non-AD.

Mice

C57BL/6 wild-type (WT) mice, 5xFAD mice and non-carrier controls (MMRRC stock #34840) were obtained from the Jackson Laboratory (Bar Harbor, ME, USA). The 5xFAD (AD) (B6SJL-Tg (APPS^wFILon, PSEN1* M146L* L286V) 6799Vas/Mmjax) mouse is a double transgenic APP/PS1 mouse model that co-expresses five AD mutations leading to accelerated plaque formation and increased A β 42 production. This AD mouse model over-expresses APP with K670N/M671L (Swedish Mutation), I716V (Florida mutation), and V717I (London mutation), PS1 with M146L and L286V mutations. These mice accumulate high levels of intra-neuronal A β -42 around 1.5 months of age with amyloid deposition around 2 months (27, 28). The adult *Atg5*^{-/-} mice were obtained from Herbert W. Virgin from Washington University with permission of Noboru Mizushima (29). All animal experiments were performed according to protocols approved by the Animal Care and Use Committee (IACUC) of the Ohio State University College of Medicine.

Perfusion of Mice

Mice were anesthetized using ketamine/xylazine mixture and perfused as described before (30). Briefly, heart was surgically exposed, and a perfusion needle was inserted directly into the left ventricle. Perfusion needle was secured in the left ventricle by using a hemostat surgical clamp. An incision was made in the right atrium to create an open circulation. First, heparinized sterile PBS was injected to flush the blood out of the circulation. This was followed by the injection of 4% paraformaldehyde (PFA) fixative solution (30). The brains were dissected and then underwent post-perfusion fixation overnight at 4°C in 4% PFA. Brains were then transferred to 30% sucrose (w/v)-PBS. Brains were embedded in Optimal cutting temperature compound (OCT) and sectioned using a cryostat. Cryosections of 15–20 microns thickness were mounted on glass slides.

Immunohistochemistry (IHC) for Mouse Tissues

Immunofluorescence (IF) staining of mouse brain sections was performed as previously described (31). Slides were washed 3 times for 15min with PBS to remove residual OCT. The sections were then incubated in the blocking solution (PBS containing 10% donkey serum (cat no: S30-100ml, Millipore Sigma), 2% BSA (Fisher Scientific, BP1600-100) and 0.3% Triton X-100 (Fisher Scientific, BP151-100) for 2h at room temperature (RT). Sections were then transferred to blocking solution containing the primary antibodies (NBR1 (proteintech, 16004-1-AP), IBA1 (Novus Biologicals, NB100-1028), and incubated overnight at 4°C. After that, sections were washed with PBS 3 times for 15min each. Then, they were incubated with the

blocking solution containing the secondary antibody Donkey anti-Rabbit IgG (ThermoFisher Scientific, A32790), Donkey anti-Goat IgG (cat. no: A-11058, ThermoFisher Scientific) for 2h at RT. DAPI (Fisher Scientific, D1306) was added on the top of the antibody solution in the last 15min of the incubation period at a final concentration (5 μ g/ml). Finally, sections were washed with PBS 3 times for 15min. Antifade mounting media (ThermoFisher Scientific, P36934) was added before cover-slipped.

Confocal Imaging of Mouse Tissue Sections and Imaris Analysis

Fluorescent images were captured on Olympus FV3000 inverted microscope with a motorized stage using 60x/1.4 NA oil objective. Images were taken at z-sections of 0.5 μ m intervals by using the 488nm, 543nm, and 405nm (for DAPI) lasers. Image reconstructions of z-stacks were generated in Imaris software (Bitplane, Inc.). Volume of NBR1 was analyzed using surface functions and masking tools as described before (32, 33). The measurement of volume was used to evaluate the amount of the target protein in 3D images. Briefly, IBA1 and NBR1 were 3D reconstructed using the Imaris surface function. Surface masking tool was used to create a new channel of NBR1 only confined to the IBA1 positive microglia. Surface function was used for the 3D reconstruction of the microglia NBR1 from the newly created channel. Subsequently, volume statistics were extracted from the 3D reconstructed surfaces. Staining and imaging were performed on 3 brains isolated from 5xFAD mice and 3 brains of age- and sex-matched WT littermates.

Immunohistochemistry (IHC) and *In Situ* Hybridization (ISH) of Human Tissues

The human brain tissues were equally divided between the hippo- campus and frontal or parietal cortex. All samples were de-identified from the patient's name, hospital where autopsy was performed, and date of birth (though birth year was maintained). The formalin fixed, paraffin embedded tissues were prepared as per standard operating procedures (entire brain fixed for two weeks, then 1 cm sections embedded in formalin). The tissue was sectioned at DLS: 4-micron sections were placed onto sequentially labeled PLUS slides, baked at 60°C for 30min, then stored in a light tight box at RT. In situ hybridization (ISH) was done using the Leica Bond Max automated platform (Leica, Buffalo Grove, IL) with the modification of substituting the Polyview polymer-peroxidase conjugate from Enzo Life Sciences (Farmingdale, NY) (26). IHC was performed for NBR1, TMEM-19, GFAP and Pyruvate dehydrogenase. The tissues were also tested for A β (1-42) after protease digestion (proteinase K solution, Enzo Life Sciences) for 4min at RT. Each antibody was from abcam and used at a dilution of 1:700.

Human Brain Section Imaging and Analysis

The imaging microscope was from Ventana Biosystems and was a Zeiss Axio Imager M1. Co-expression analyses were done using the Nuance/InForm software (Perkin Elmer) whereby each chromogenic signal is separated, converted to a fluorescence-

based signal, then mixed to determine what percentage of cells were expressing the two proteins of interest as previously described. The number of positive cells/200X field was counted with the InForm software or manually. Manual and InForm computer-based counts were found to be equivalent.

A β Peptides and Fibrillization

A β peptides in powder form (Anaspec) were initially resuspended in 1% NH₄OH for 15min to dissolve any pre-formed aggregates per manufacturer instructions, and then diluted to a final concentration of 0.05% NH₄OH in water prior to fibrillization. A β peptides were converted to the fibrillar form of A β by incubating monomeric human A β (1-42) (cat. no: AS-20276) or human Hilyte Fluor 555 labeled A β (1-42) (cat. no: AS-60480-01) at 220 μ M in water at 37°C for 3days prior to use as previously described (34). Hilyte Fluor is more photostable than the classic fluorescent dyes. They are also highly fluorescent over a broad pH range with little pH sensitivity (Anaspec). Treatment with 1 μ M A β was completed in serum free media for 1h before washing away excess A β and adding full media.

Microglial Isolation and Culture

Microglia were isolated by MACS neural dissociation kit (Miltenyi Biotec, 130-107-677) followed by CD11b magnetic bead (Miltenyi Biotec, 130-093-634) isolation technique to positively select for microglia expressing the pan-microglial marker CD11b as has been described before (35). For experiments evaluating 5xFAD microglia in culture, microglia were isolated from adult mice between 4-6-months-old and age- and sex-matched WT littermate mice. For experiments evaluating WT and *Atg5*^{-/-} mice, microglia were isolated from 2-3-month-old mice. Genotypes were age- and sex-matched. For experiments using WT mice, brains from 2 mice were combined as one biologic replicate. For experiments using AD mice, one brain was sufficient per biologic replicate. Experiments with microglia in culture were performed on 3 or 4 unique biologic replicates as indicated. Experiments were performed using both female and male mice. No trends in the data were observed based on sex. Microglia were then cultured on either 24-well plates with pre-coated cover slips with 0.005% Poly-L-lysine (Sigma, P4707) at 2x10⁵ microglia per coverslip. Microglia were cultured in IMDM media (ThermoFisher Scientific, 12440053) supplemented with 10% of heat inactivated fetal bovine serum (FBS) (ThermoFisher Scientific, 16000044), 50% L cell-conditioned media, 0.6x MEM Non-Essential Amino Acids (ThermoFisher Scientific, 11140050) and 0.1% penicillin and streptomycin (Thermo Fisher Scientific, 15140122).

Fluorescent A β (1-42)-555 Degradation Assay and Image Analysis

Primary microglia were plated at 2x10⁵ cells per well on glass coverslips. Two wells from the same biological replicate were treated with 1 μ M Hilyte Fluor 555 labeled fibrillar A β (1-42) for 1h in serum free media. Un-internalized A β (1-42) was removed by rinsing with warm full media. One coverslip was fixed with 4% PFA after an additional 2h. The other well was incubated for 48h

prior to PFA fixation. Prior to fixation, cells were stained with Hoechst 33342 for 10min (ThermoFisher Scientific, 62249). Images were acquired by confocal microscopy and analyzed for volume of A β (1-42)-555 and number of cells by Imaris software. Volume of Fluor A β was normalized to the number of cells for each time point (Degradation % = [(Volume A β at 3h/cell number - Volume A β at 48h/cell number)/(Volume A β at 3h/cell number)] \times 100). Fluorescent images were captured on Olympus FV3000 inverted microscope with a motorized stage using 10x objective. Images were acquired at z-sections by using 543nm, and 405nm (for DAPI) lasers. Imaris software was used to generate projection images and for analysis. Volume of Fluor A β (1-42)-555 was calculated using surface function. Background subtraction function was also used to enhance IF Signal-To-Noise-Ratios (32, 33). Number of cells was counted using spots function in the DAPI channel.

Down-Regulation of *miR-17* in Primary Microglia

50nM miRNA inhibitor to *miR-17-5p* (antagomir17) (ThermoFisher Scientific, 4464084), or negative inhibitor control (ThermoFisher Scientific, 4464079) were transfected into microglia utilizing the Hiperfect transfection system (Qiagen, 301704) in full media according to the manufacturer's instructions for 48h prior to performing treating with A β .

LC3 and NBR1 Immunofluorescence of Primary Microglia and Image Analysis

Primary microglia were plated at 2x10⁵ cells per well on glass coverslips overnight. Microglia from 5xFAD mice were treated with antagomir-17 or negative control as described where indicated. The cells were washed once with warm media and then the assigned wells were treated with 1 μ M Hilyte Fluor 555 labeled fibrillar A β (1-42) for 1h prior to washing all the wells 3 times with warm media. The cells were then fixed with 4% PFA either after 2, 4, 6h as indicated for 20min before washing 3 times with PBS. The fixed cells were permeabilized and blocked by incubating in blocking solution (PBS containing 10% donkey serum, 2% BSA and 0.3% Triton X-100) for 2h at RT. They were then transferred to blocking solution containing the primary antibody LC3 (Cell Signaling Technology, 12741) or NBR1 (Proteintech, 16004-1-AP) and incubated overnight at 4°C followed by PBS wash 3 times. The cells were then incubated with the blocking solution containing the secondary antibody goat anti-Rabbit IgG (Thermofisher scientific, A11008) for 2h at RT. Cell nuclei were stained with 5ug/ml DAPI. Antifade mounting media was added before cover-slipped. The Images were taken at z-sections (12 images per cover slip for LC3 and 10 per coverslip for NBR1) of 1 μ m intervals by using the 488nm, 543nm, and 405nm (for DAPI) lasers. Image reconstructions of z-stacks were generated in Imaris software (Bitplane, Inc.). For LC3 quantification, LC3 volume was analyzed using surface function as described before (32, 33). The measurement of volume was used to evaluate the amount of the target protein in 3D images. For NBR1 positive cells quantification, microglia that express 3 or more NBR1 puncta was manually counted in a blinded manner. Cells were considered positive for NBR1 puncta

if they met the selected threshold of 3 puncta. Assigning an appropriate threshold for counting puncta for autophagy studies is discussed in the guidelines for monitoring autophagy report (36).

A β Degradation in HMC3 Microglia

Human microglia cell line (HMC3) was purchased from ATCC (CRL-3304) and cultured in MEM (ThermoFisher scientific, 11995040), supplemented with 10% FBS. Cells were plated at 1×10^5 cells per well in 12 well plate. Transfection was performed in Opti-MEM media (Gibco, 31985070) with NBR1 sirna (Dharmacon, LQ-062130-01-0005) or its non-targeting negative control next day for 24h before treatment with $1 \mu\text{M}$ fibrillar A β (1-42) for 1h. Then, the cells were washed 3 times with PBS, and media was replaced. Cells were lysed at 4 and 24h with TRIzol. Protein extraction and immunoblotting for A β were performed to assess the course of A β degradation.

Immunoblot

Protein extraction was performed using TRIzol reagent (Invitrogen Life Technologies, 15596026) according to the manufacturer's instructions. Briefly, after phase separation using chloroform, 100% ethanol was added to the interphase/phenol-chloroform layer to precipitate genomic DNA. Subsequently, the phenol-ethanol supernatant was mixed with isopropanol to isolate proteins. The Bradford method was used to determine protein concentrations. Equal amounts of protein were separated by 13.5% SDS-PAGE and transferred to a polyvinylidene fluoride (PVDF) membrane. Membranes were incubated overnight with antibodies against mouse NBR1 (Cell Signaling Technology, 9891S), human NBR1 (Proteintech, 16004-1-AP), human beta-amyloid (Cell signaling technology, 8243S), ATG5 (Cell Signaling Technology, 12994S), ATG7 (Cell Signaling Technology, 8558S), Beclin 1 (Cell Signaling Technology, 3495S) and GAPDH (Cell Signaling Technology, 2118). Corresponding secondary antibodies conjugated with horseradish peroxidase and in combination with enhanced chemiluminescence reagent (Amersham, RPN2209) were used to visualize protein bands.

Quantitative Real-Time PCR (RT-qPCR) for Expression of *MiRs* and Autophagy Genes

Total RNA was isolated from cells that were lysed in TRIzol. Chloroform (cat no: 268320010, Fisher Scientific), isopropanol (cat no: BP2618212, Fisher Scientific), and glycogen (cat no: 10814010, Fisher Scientific) were used to isolate total microglia RNA and its concentration was measured by Nanodrop. The expression of different *MiRs* and autophagy genes was determined as previously described and expressed as relative copy numbers (RCN) (37). Ct values of each gene or *MiR* were subtracted from the average Ct of the internal control. The resulting ΔCt was used in the equation: $\text{RCN} = (2^{-\Delta\text{Ct}})$.

Intracisternal Magna (ICM) Injection of Antagomir-17

To determine the impact of blocking action of *miR-17*, mice received an infusion of antagomir-17 (mirVana miRNA

inhibitor; 4464088, ThermoFisher) or non-targeting control (4464077) into the cisterna magna (ICM) as described previously (38, 39). Four mice were injected with non-targeting control (3 males and 1 female) and 3 mice were injected with antagomir-17 (2 males and 1 female). The inhibitor and non-targeting control was prepared for *in vivo* ready use by the manufacturer. Mice were briefly anesthetized with isoflurane and the dorsal aspect of the skull was shaved. A 27-gauge needle attached *via* PE50 tubing to a 25 μl Hamilton syringe was inserted into the cisternal magna. To verify entry into the cerebral spinal fluid (CSF), approximately 2 μl of clear CSF was drawn and gently pushed back in and 4 μl of antagomir-17 (dose of 1.2 nmole) was slowly administered and allowed to absorb for 1 min before the needle was removed. Following injection, isoflurane was immediately discontinued and mice were awake, alert and mobile within 3min. Mice were injected once weekly for 4 weeks and then euthanized after 1 more week to isolate microglia by CD11b(+) magnetic bead purification. Microglia were isolated and immediately lysed in TRIzol. ICM injections were utilized as no surgery or cannulae implantation are required, which are inflammatory manipulations, and because substances injected ICM spread readily throughout the central nervous system (CNS) (38).

Statistical Analysis

All figures display mean and standard error of the mean (SEM) from at least three independent experiments as indicated in the figure legends. Comparisons between groups were conducted with either two-sample t-test, one-way or two-way ANOVA (depending on the data structure) for independent data, but with linear mixed effects models for correlated data to take account of the correlation among observations obtained from the same subject. Holm's adjustment for multiple comparisons was used as indicated. Adjusted $P < 0.05$ was considered statistically significant.

RESULTS

Microglial Autophagy Is Required for Degradation of A β , but Autophagy Proteins Are Poorly Expressed in 5xFAD Microglia

There are no studies using primary microglia *in vitro* from adult AD mouse models to determine their ability to degrade A β . Therefore, we sought to determine if microglia from 4-6-month-old 5xFAD mice in culture exhibit reduced degradation of fibrillar A β , the form most commonly found in plaques (2). The 5xFAD mouse model of AD expresses 5 mutations seen in familial forms of AD under the Thy1 neuronal promoter (27). This model exhibits robust deposition of A β , starting at 2-months of age, followed by microgliosis and loss of cognitive function between 4-6 months (27). WT and 5xFAD microglia were isolated by CD11b magnetic bead separation, plated, and then treated with fluorescent A β ($1 \mu\text{M}$ labeled with acid-resistant Hilyte Fluor 555) for 3 or 48 hours. A β degradation (%) was calculated by measuring reduction in fluorescent-A β volume

between 3 and 48 hours per cell number. We found that microglia cultured from brains of 6-month-old 5xFAD mice are less able to degrade A β when compared to their WT counterparts (**Figures 1A, B**).

To determine if autophagy contributes to A β degradation and clearance in primary adult microglia, microglia from *Atg5*^{-/-} mice were isolated. ATG5 is necessary for elongation of autophagic membranes and enables the recruitment of autophagy molecule LC3. We performed a fluorescent-A β degradation assay comparing *Atg5*^{-/-} and WT microglia. We found that *Atg5*^{-/-} microglia were less capable of A β degradation than WT microglia at 48 hours (**Figures 1C, D**). To confirm that primary adult microglia traffic A β *via* autophagy, we treated WT microglia with fluorescent-A β for 2 and 6 hours and stained for LC3 which is an important marker of autophagosomes. We found that LC3 volume increases upon addition of A β (**Figures 1E, F**). Moreover, it colocalizes with A β and colocalization increased between 2 and 6 hours (**Figures 1E, G**). Overall, these results indicate that healthy microglia are capable of enclosing A β into an autophagosome and degrading it by employing functional autophagy.

To determine the underlying defect responsible for failed autophagy-mediated degradation of A β in AD microglia, we determined autophagy protein expression in microglia from 5xFAD mice. Microglia were isolated from 5xFAD mice and age- and sex-matched WT littermates at both 2- and 6-month-old as significant A β deposition and microgliosis occurs after 2 months (27). Microglia were purified by magnetic bead positive selection for CD11b and the CD11b-negative fraction was also collected. By immunoblot analysis, expression of autophagy proteins NBR1, ATG7, BECN1, and ATG5 were analyzed in both the microglia and non-microglial fractions (**Figures 2A, B**). NBR1 and ATG7 were significantly less expressed in microglia in 6-month-old 5xFAD mice. This difference was not observed at 2 months, indicating that the expression of autophagy proteins is downregulated in microglia over the course of the disease (**Supplementary Figures 1A, B**). Expression of both *Nbr1* and *Atg7* mRNA was also diminished in 6-month-old (not 2-month old) 5xFAD mice (**Figure 2C**). We did not observe differential expression of ATG5 or BECN1 (**Figures 2A, B**) or any autophagy markers in the microglia fraction of 2-month-old mice (**Supplementary Figures 1A, B**). However, NBR1 and ATG5 were elevated at 2-months in the non-microglia fraction, though the difference disappeared in older mice. The results in **Figures 2A, B** show that the expression of NBR1 is decreased in 5xFAD microglia purified from the brain. Since transcriptional changes may occur during both isolation and culture of microglia (40), we characterized the expression of NBR1 in microglia *in situ*. To do this, NBR1 expression in microglia was analyzed using immunofluorescence staining in 5xFAD hippocampal brain sections from 6-month-old 5xFAD mice. Microglia in 5xFAD mice exhibited significantly lower expression of NBR1 protein (**Figures 2D, E**) compared to WT microglia. Together, these results indicate that degradation of A β in 5xFAD microglia is compromised due to diminished expression of autophagy molecules NBR1 and ATG7. Our data

also demonstrate that autophagy is necessary for A β degradation in microglia.

Autophagy-Cargo Receptor NBR1 Is Poorly Expressed in Microglia of Human Alzheimer's Disease in Areas With A β -Deposits and Is Necessary for A β Degradation by Microglia

Autophagy linker molecules such as p62 and NBR1 bind to labeled cargo destined for autophagy and recruit LC3 and the nascent autophagosome (15). We hypothesized that NBR1 plays a critical role in autophagic degradation of A β , as its expression was diminished in microglia isolated from the brains of 5xFAD mice. To determine if this is the case in AD human subjects, we first examined expression of NBR1 in total human brain tissue homogenates. We obtained snap-frozen brain tissue sections (Brodmann Area 38) from deceased AD patients that were homogenized in TRIzol (characteristics of patients and age- and sex-matched controls can be found in **Supplemental Table 1**). We found that NBR1 protein and mRNA expression were not altered in total brain homogenates from AD human patients compared to no-disease controls (**Supplemental Figures 2A–C**). We hypothesized that NBR1 expression is reduced in specific cell populations so that total brain tissue would obscure these results. We analyzed formalin fixed, paraffin embedded human temporal lobe brain tissue sections from AD and non-AD patients and stained for specific cell populations. Microglia (TMEM+) and neurons (Pyruvate Dehydrogenase+) expressed almost no NBR1 in AD brains in comparison to non-AD which expressed a significant amount of NBR1 (**Figures 3A, B**). In contrast, astrocytes (GFAP+) in AD expressed significantly more NBR1 than in non-AD. We next analyzed regions in the AD brain with intense A β deposits build-up, to determine if NBR1 down-regulation is associated with A β deposits burden. Microglia in tissue sections with A β -deposits had lower expression of NBR1 compared to microglia away from A β deposits (**Figures 3C, D**). These results indicate that NBR1 down-regulation is specific to microglia and neurons in AD, particularly in regions with intense A β deposition.

To determine if NBR1 is required for A β degradation, the human microglia cell line HMC3 was transfected with *NBR1* siRNA or non-target control, leading to successful knockdown of NBR1 at protein and mRNA level (**Figures 4A–C**). We then performed an A β degradation assay by immunoblot and discerned that microglia with low NBR1 expression degraded less A β at 24 hours when compared to NBR1-expressing microglia (**Figures 4D, E**). These data indicate that NBR1 is necessary for A β clearance, however a mechanism behind its low expression in AD microglia remained elusive.

The Mirc1/Mir17-92 Cluster Is Upregulated in Microglia of Human Alzheimer's Disease in Areas With A β -Deposits

To determine the mechanism underlying reduced expression of NBR1, we searched for MicroRNAs that are predicted to target

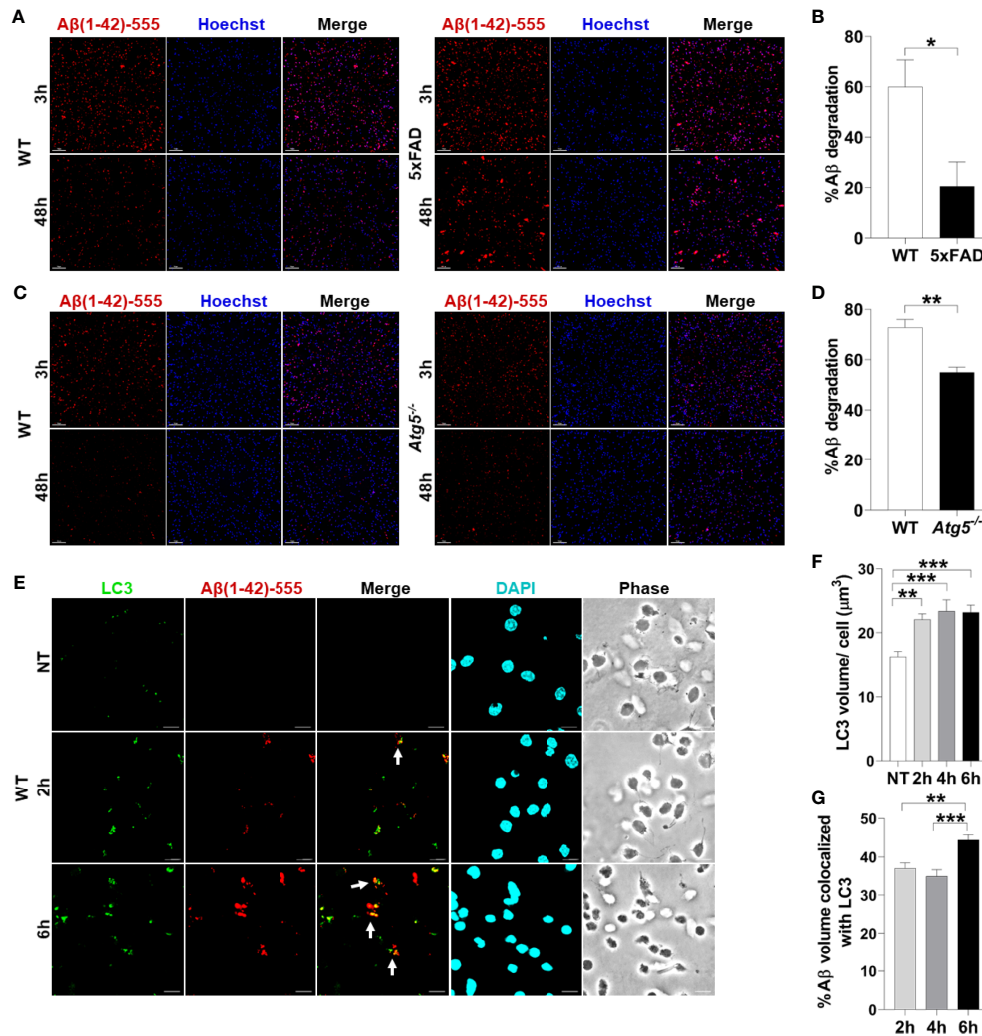


FIGURE 1 | A β degradation is diminished in 5xFAD microglia and autophagy knockout microglia. **(A)** Representative confocal images of fluorescent-A β (red) in primary microglia isolated from 4-6-month-old 5xFAD and sex- and age-matched WT littermate's brains treated with A β for 3 or 48h. Scale bar: 10 μ M. **(B)** Quantification of degradation of fluorescent-A β (red) by degradation assay of the images represented in **(A)** ($n = 3$). Values are % of A β volume reduction \pm SEM calculated by scoring 5 randomly chosen 20x fields of view per biologic replicate. Statistical analysis was performed using unpaired two tailed Student's t-test. **(C)** Representative confocal images of fluorescent-A β (red) added to primary microglia isolated from 2-3-month-old WT and *Atg5*^{-/-} mice' brains for 3 and 48h. Scale bar: 10 μ M. **(D)** Quantification of images represented in **(C)** were completed as described in **(B)** ($n=3$). Statistical analysis was performed using unpaired two tailed Student's t-test. **(E)** Representative confocal images of LC3 (green) in fluorescent-A β (red) treated primary WT microglia for 2,6h. Colocalization is represented in yellow as indicated by arrows. **(F)** Quantification of LC3 volume from cells treated as in **(E)** for 2,4,6h performed using Imaris software ($n = 4$) (12 images per biologic replicate). Statistical analysis performed by matched one-way ANOVA. **(G)** Quantification of LC3 A β colocalization from cells treated as in **(E)** for 2,4,6h performed using Imaris software ($n = 4$) (12 images per biologic replicate). Statistical analysis performed by matched one-way ANOVA. * $p \leq 0.05$, ** $p \leq 0.01$, *** $p \leq 0.001$.

NBR1 and are highly expressed in AD. As members of the Mirc1/Mir17-92 cluster target essential autophagy molecules (24), the expression of the Mirc1/Mir17-92 cluster was evaluated in TRIzol-homogenized brain tissue (Brodmann Area 38) from deceased AD patients. Expression of each member of the cluster, especially *miR-17*, was significantly increased compared to the age-matched non-AD samples (**Figure 5A**). Additionally, the distribution of *miR-17* in fixed brain tissue sections from AD patients and age- and gender-

matched controls were analyzed by ISH. Non-AD brains showed low levels of *miR-17* in comparison to AD brains which expressed abundant *miR-17* (**Figures 5B, C**).

To discern the location of highly expressed *miR-17*, we utilized combined ISH and immunohistochemistry (IHC) to determine if the elevation of *miR-17* correlated with the presence of A β . We found that the expression of *miR-17* was elevated in areas adjacent to A β deposits but not in other sections without deposits from the same AD patient (**Figures 5D, E**).

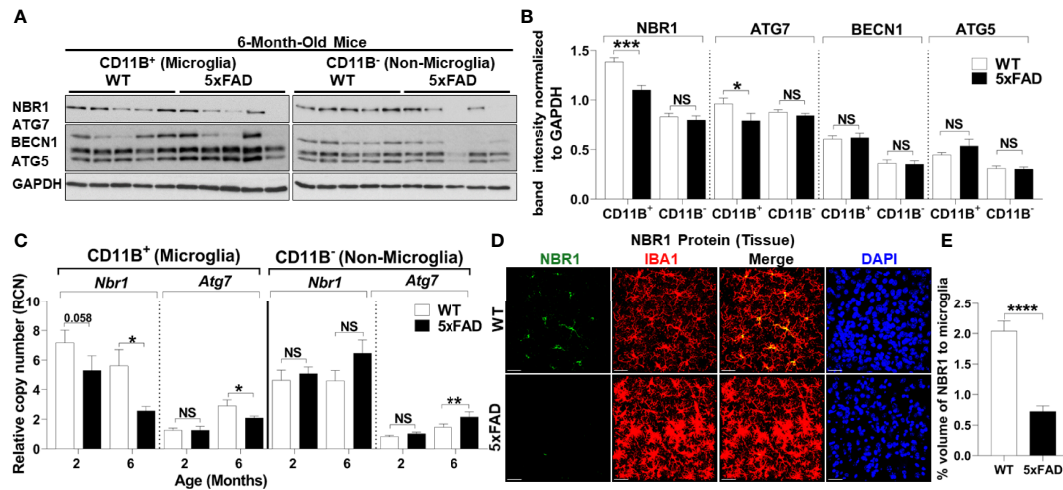


FIGURE 2 | 5xFAD microglia exhibit reduced expression of NBR1 and to a lesser extent Atg7 autophagy proteins at 6 months. **(A)** NBR1, ATG7, BECN1, ATG5 and GAPDH immunoblot of primary microglia (CD11b⁺) and non-microglia (CD11b⁻) fractions of 6-month old 5xFAD and sex- and age-matched wild-type (WT) littermate brains (n = 5). **(B)** Densitometry analysis of immunoblots represented in **(A)**. Data represent mean \pm SEM (n = 5). Statistical analysis was performed using unpaired two-tailed student's t-test. **(C)** Relative copy number of *Nbr1* and *Atg7* in primary microglia (CD11b⁺) or non-microglia (CD11b⁻) fractions of 2 and 6 month old 5xFAD and sex- and age-matched wild-type (WT) littermate brains (n = 9 for 2 month and n = 12 for 6 month). Statistical analysis was performed using mixed-effect analysis. **(D)** Representative confocal images of NBR1 protein (green) expression on brain tissue sections stained for IBA1 + microglia (red) from 6-month old 5xFAD and age-matched WT littermates. **(E)** Quantification of images represented in **(D)** was analyzed by Imaris software (n = 3). Statistical analysis was performed by unpaired student t-test. *p \leq 0.05, **p \leq 0.01, ***p \leq 0.001, ****p \leq 0.0001, NS, Not Significant.

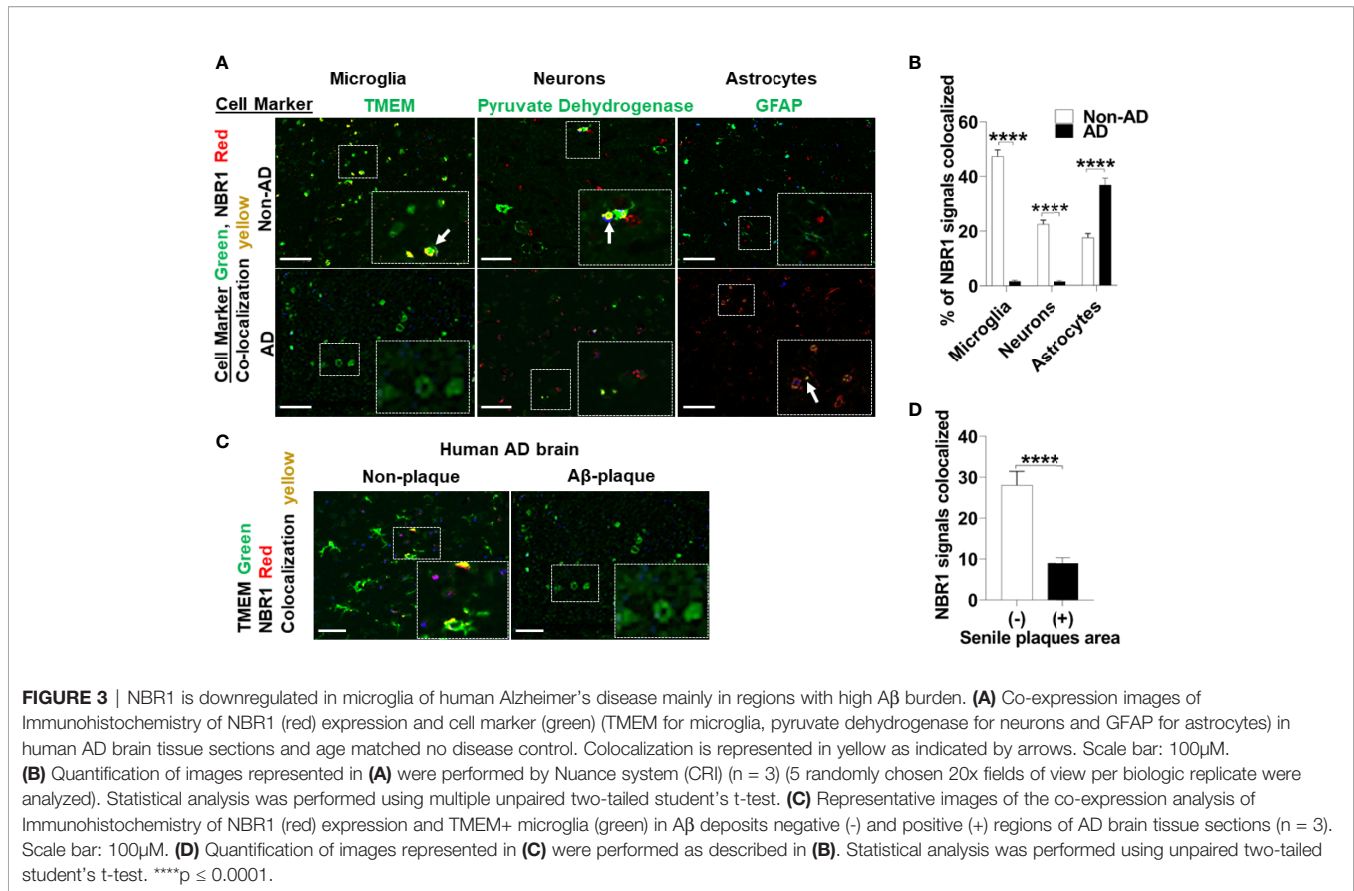
Microglia are known to robustly proliferate at the site of A β deposition (41). Since *miR-17* is highly expressed in regions where A β accumulates, we tested if the upregulation of *miR-17* occurs specifically in microglia. By using combined ISH/IHC we evaluated expression of *miR-17* with co-staining for microglia (TMEM⁺) in AD brain sections. We observed that approximately 45% microglia adjacent to A β deposits highly expressed *miR-17* (Figures 5F, G). We also analyzed neurons (pyruvate dehydrogenase⁺) and found that approximately 50% of neurons expressed *miR-17* (Figure 5G). Only regions with A β deposits in AD brains were analyzed by cell type as both non-AD samples and non-A β deposit regions did not express any *miR-17* (Figures 5B–E). We concluded that both microglia and neurons in the vicinity of A β deposits express *miR-17* in human AD brain. Therefore, *miR-17* may alter expression of specific protein targets in both of these cell types in the AD brain.

To test if microglia in 5xFAD mice express significant levels of all the members of the Mir1/Mir17-92 cluster compared to their age-matched WT littermates, microglia were isolated from 6-month-old 5xFAD mice utilizing CD11b magnetic-bead purification. We analyzed both the CD11b (+) microglia fraction and the remaining CD11b (-) non-microglia fraction for the Mir1/Mir17-92 cluster by RT-qPCR. We found that the members of the cluster are upregulated in isolated microglia, but not in the non-microglia fraction (Figure 6A). The non-microglia fraction contains all cell types collected together, such as neurons, and other glia cells including astrocytes, oligodendrocytes and ependymal cells. As different cell types are analyzed together, the elevation of *miR-17* in a specific cell, such as in neurons as seen in human AD (Figure 5G), could be

masked by other cells that do not express *miR-17*. Since A β deposition starts to occur in the 5xFAD mouse after 2 months, we tested if the elevation of the cluster in 5xFAD microglia occurs by the age of 2 months. We purified microglia from 2-month-old 5xFAD mice and WT littermates and found no detectable difference in cluster expression in microglia or non-microglia (Figure 6B). Overall, we identified upregulation of the Mir17-92a cluster in both human and mouse AD microglia, which may contribute to dysfunctional autophagy and failed clearance of A β .

Inhibition of Upregulated *miR-17* Is Sufficient to Restore the Ability of 5xFAD Microglia to Degrade A β

We hypothesized that treatment with an inhibitor of *miR-17* (antagomir17) would restore the ability of 5xFAD microglia to degrade A β *in vitro*. *MiR-17* is highly expressed in AD microglia in human and mouse microglia and is known to target multiple autophagy effectors (24). To detect if 5xFAD microglia in culture lose the differential expression of Mir1/Mir17-92 cluster, expression of this cluster was analyzed after 24 hours in culture in full media. We found that 5xFAD microglia compared to age-matched littermates still exhibit increased expression of the cluster (Supplemental Figure 3). To determine if reducing expression of *miR-17* in AD microglia improves the degradation of A β , 6-month-old 5xFAD microglia were transfected with antagomir-17 or non-target negative control. A fluorescent-A β degradation assay was performed after 48 hours of antagomir-17 or negative inhibitor transfection. Treatment with antagomir-17 significantly



improved A β degradation (**Figures 6C, D**). Our data indicate that inhibition of *miR-17* alone is sufficient to significantly improve the degradation of A β in 5xFAD microglia *in vitro*. Therefore, targeting all members of the cluster to improve A β degradation is not necessary.

To determine if improved A β degradation after *miR-17* inhibition is due to recovered autophagy function, 5xFAD microglia were probed for autophagosome marker LC3 after 48 hours of antagomir-17 or negative control transfection. Microglia were treated with A β for 2 hours to observe differences in LC3 accumulation after A β degradation. Similar amounts of A β were associated with microglia treated with antagomir-17 or the negative control after 2 hours (**Figures 6E, F**). Notably, microglia treated with antagomir-17 exhibited increased LC3 volume compared to the negative control, indicating increased presence of autophagosomes (**Figures 6E, G**).

We demonstrated that NBR1 is involved in A β degradation and that *miR-17* prevents degradation of A β in AD microglia. Importantly, DIANA-TarBase v8 (42), a reference database indexing experimentally supported *MiR* targets, validated NBR1 as a target of *miR-17* (43). Therefore, we quantified NBR1 puncta formation in AD microglia after inhibition of *miR-17*. NBR1 puncta represent receptor clustering which promotes continued autophagosome formation (44). Counting puncta labeled with various autophagy proteins is routinely used in autophagy studies to provide a snapshot of this dynamic

process (45). We then examined if AD microglia treated with antagomir-17 would express more NBR1 puncta than the negative control treated microglia. 5xFAD microglia were probed for NBR1 after 48 hours of antagomir-17 or negative control transfection. Microglia were then treated with A β for 2 hours to observe differences in NBR1 accumulation before detectable A β degradation starts. Cells were considered positive for NBR1 if they met the threshold of 3 puncta per cell. We found that significantly more AD microglia treated with antagomir-17 were positive for NBR1 puncta compared to cells treated with the negative control (**Figures 6H, I**). Taken together, these results indicate that inhibition of *miR-17* improves A β degradation, autophagy and NBR1 puncta formation in 5xFAD microglia.

Targeting *miR-17* *In Vivo* Improves the Expression of NBR1

We speculated that reducing the expression of *miR-17* would also bolster the expression of NBR1 *in vivo*. To confirm that antagomir-17 treatment *in vivo* would effectively increase autophagy protein expression in microglia, we injected 5xFAD mice with 1.2 nmole of antagomir-17 once weekly for four weeks by intracisterna magna (ICM) injection. Both the CD11b (+) and CD11b (-) fractions were collected for analysis. Mice treated with antagomir-17 had significantly higher levels of NBR1 in both microglia and the CD11b (-) fraction compared to the non-targeting control (**Figures 7A, B**). We also analyzed expression

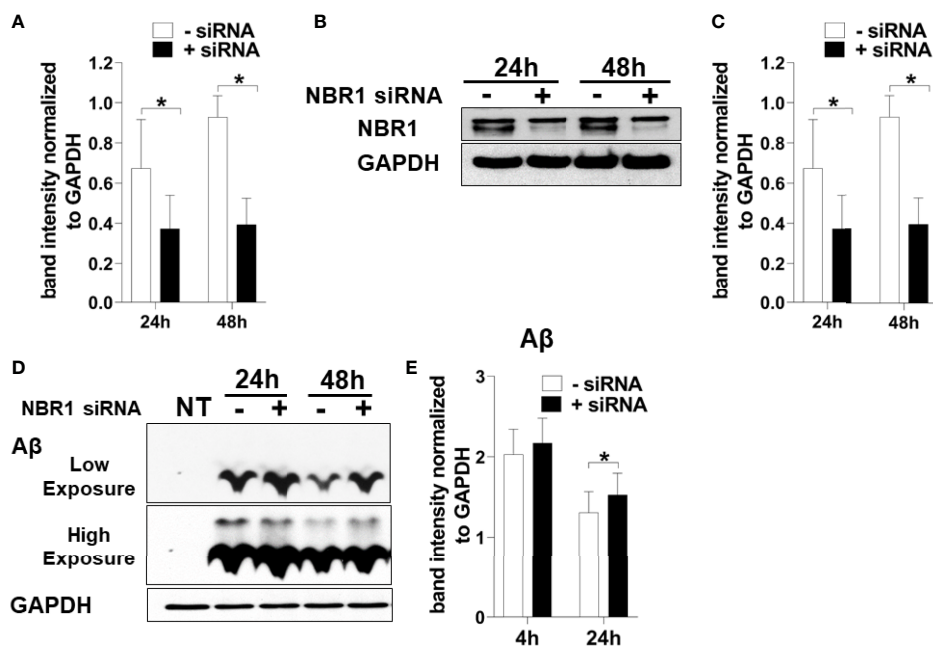


FIGURE 4 | NBR1 is required for A β (1-42) degradation. **(A)** *Nbr1* relative copy number in human microglial cell line (HMC3) treated with 50nM *Nbr1* siRNA or non-targeting negative control for 24 and 48h ($n = 4$). Statistical analysis performed using paired two tailed Student's t-test. **(B)** NBR1 and GAPDH immunoblot of HMC3 cells treated as in **(A)** ($n = 4$). **(C)** Densitometry analysis of immunoblots represented in **(B)**. Data represent mean \pm SEM ($n = 4$). Statistical analysis performed using paired two-tailed student's t-test. **(D)** Immunoblot for A β and GAPDH in HMC3 microglia transfected as in **(A)** for 24h and treated with 1 μ M of fibrillar A β (1-42) for either 4 or 24h to assess the course of A β degradation. **(E)** Densitometry analysis of immunoblots represented in **(D)**. Data represent mean \pm SEM ($n = 4$). Statistical analysis was performed using matched two-way ANOVA. * $p \leq 0.05$.

of ATG7, ATG5 and BECN1 (**Figures 7A, B**). We noted a modest, though non-significant, improvement in ATG7 expression in microglia after antagomir-17 treatment. Additionally, we determined that ATG5 and ATG7 expression were improved in non-microglial cells after antagomir-17 treatment. In order to determine if decreased expression of NBR1 in human AD correlates with increased expression of *miR-17*, a correlation analysis was performed utilizing combined ISH/IHC. First, we performed this analysis in the AD brain in regions with and without A β deposits (**Figure 7C**). Decreased expression of NBR1 was highly correlated with increased expression of *miR-17* (**Figure 7D**). Additionally, we completed this analysis on AD brains with deposits together with no-disease controls. Decreased expression of NBR1 was highly correlated with increased expression of *miR-17* (**Figure 7E**). Overall, our results indicate that in AD, the overexpressed *miR-17* correlates with reduced expression of NBR1 which participates in the A β degradation in microglia. A schematic illustration of the interplay between *miR-17*, NBR1 and A β degradation in both healthy and Alzheimer diseased microglia is suggested in (**Figure 8**).

DISCUSSION

Healthy microglia play a crucial role in clearing A β deposited by neurons in the brain (8). However, microglia become

dysfunctional over the course of AD and fail to clear A β , and instead they release toxic neuro-inflammatory products (10). Degradation of A β can be mediated by microglia by various mechanisms, including release of extracellular enzymes such as neprilysin or insulin-degrading enzyme or by degradation of A β following phagocytosis where internalized cargo is delivered to phagolysosomes or autophagolysosomes for degradation (6–8, 12). Previous reports suggested that autophagy machinery degrades A β following phagocytosis and that weak autophagy activity in microglia is associated with failed A β clearance and unsuccessful regulation of neuro-inflammatory phenotypes (11–13, 18, 46, 47). However, these studies were completed in neonatal microglia or microglia cell lines and did not offer underlying mechanisms for defective autophagy in AD microglia. We demonstrate for the first time using our model of primary adult mouse microglia that A β degradation following phagocytosis is dependent on autophagy and that A β colocalizes with autophagosome marker LC3. Furthermore, we demonstrate that expression of specific autophagy proteins NBR1 and to a lesser extent ATG7 are diminished in 5xFAD mouse microglia. This is the first study employing adult 5xFAD microglia where we show that NBR1 is required for A β degradation. Hence, reduced expression of NBR1 is responsible (at least in part) for failed degradation of A β by 5xFAD microglia. This is a very important finding since NBR1 is involved in early steps of autophagy degradation and hence, cannot be remedied by

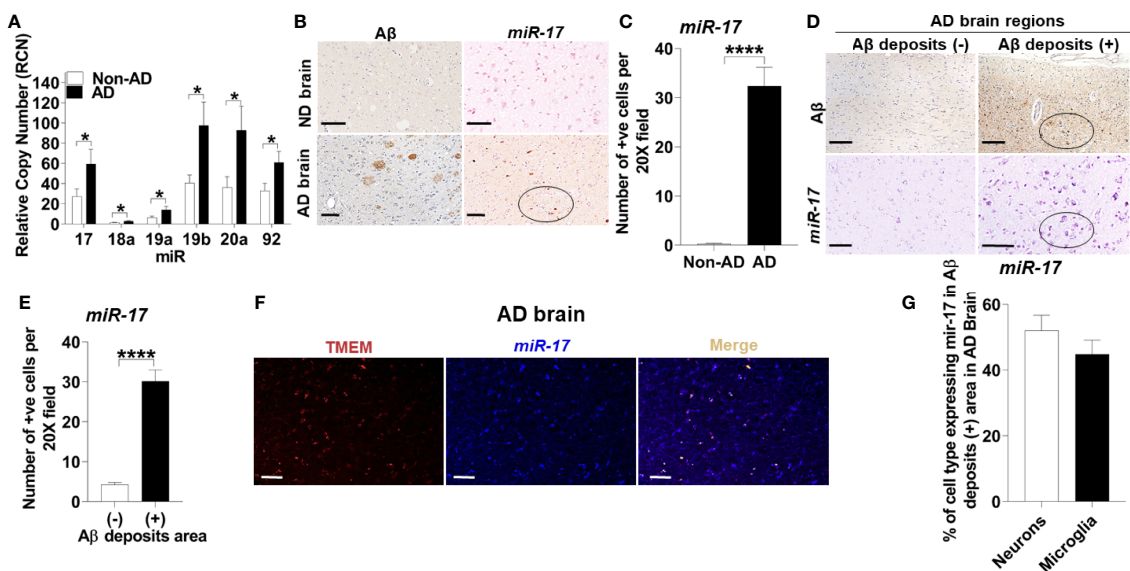


FIGURE 5 | The Mirc1/Mir-17-92 cluster is upregulated in human Alzheimer's disease and is expressed in microglia. **(A)** Relative copy number of the six miRNAs of the miR-17-92 cluster in human AD brain tissue sections and their age-matched no disease controls ($n = 15$). Statistical analysis was performed using multiple unpaired two-tailed student's t-test. **(B)** Representative images of A β deposits and *in situ* hybridization of *miR-17* in adjacent brain tissue sections of human AD and no disease control. A region with multiple *miR-17* positive cells is circled. Scale bar: 100 μ m. **(C)** Quantification of cells expressing *miR-17* represented in **(B)**. Values are mean \pm SEM calculated by scoring 3 randomly chosen 20x fields of view ($n = 4$). Statistical analysis was performed using unpaired two tailed Student's t-test. **(D)** Representative images of *in situ* hybridization of *miR-17* in A β deposits negative (-) and positive (+) area of AD brain tissue sections. Images of A β are adjacent tissue sections to corresponding *miR-17* images. A region with multiple *miR-17* positive cells and corresponding A β deposits section is circled. Scale bar: 100 μ m. **(E)** Quantification of images represented in **(D)** as described in **(C)** ($N = 4$). **(F)** Representative images of the co-expression analysis of *in situ* hybridization of *miR-17* (blue) and Immunohistochemistry of TMEM (as selective marker for microglia) (red) with merge image completed by nuance processing in an A β deposits positive area of AD brain tissue sections. Colocalization in the merge image is shown in yellow. Scale bar: 100 μ m. **(G)** Percentage of the neurons and microglia expressing *miR-17* in A β deposits positive area of AD brain tissue sections ($n = 3$). * $p \leq 0.05$, **** $p \leq 0.0001$.

increasing the expression of the downstream autophagy effectors. Moreover, we offer a mechanism underlying dysfunctional autophagy-mediated degradation of A β . Our study uncovered that the Mirc1/Mir17-92a cluster is upregulated in 5xFAD mouse and human AD microglia which is associated with decreased expression of autophagy proteins specifically NBR1. Highly expressed *miR-17* in AD microglia targets NBR1 leading to its downregulation which renders AD microglia unable to degrade A β by the autophagy machinery. We found that inhibition of *miR-17* alone improved degradation of A β , which offers a unique drug target.

MiRs are heavily implicated in both AD pathogenesis (21, 23) and autophagy (20), but there was a lack of evidence linking these two processes. Members of the Mirc1/Mir17-92 cluster negatively target expression of autophagy proteins, leading to weak autophagy activity in different disease conditions including multiple cancers and cystic fibrosis (24, 48). We discovered that the Mirc1/Mir17-92a cluster is upregulated in microglia in the temporal lobe of human AD patients compared to sex- and age-matched patients with no known dementia. These findings are distinct from previous studies describing downregulated expression of the Mirc1/Mir17-92 cluster during aging and senescence using total brain homogenates (25).

We observe elevated expression of *miR-17* in microglia and neurons in human AD adjacent to A β deposits. Several reports

suggest that dysfunctional autophagy in AD neuronal cells contributes to the over-production of abnormal A β and subsequent aggregation which instigates the process that leads to AD pathology (49). We also demonstrate that the Mirc1/Mir17-92a cluster is significantly upregulated in 6-month-old 5xFAD mice, which is after the detection of deposition of A β plaques in this model (27). Therefore, the dysregulation of A β deposition from neuronal cells precedes autophagy dysfunction in surrounding microglia. It is possible that long-term exposure to A β plaques provokes the upregulation of *miR-17* in surrounding cells. Yet, in our hands, exposure of non-diseased microglia to A β for several days *in vitro* did not increase the expression of *miR-17* (data not shown). Alternatively, the Mirc1/Mir17-92 cluster is consistently upregulated in highly inflammatory diseases including tumor sites and in the lungs of cystic fibrosis patients especially during pulmonary exacerbations (50). Therefore, it seems that the deposition of A β plaques in the AD brain instigates micro-environmental effects that collectively lead to the upregulation of the cluster and disruption of autophagy in microglia, which requires further investigation. Notably, we report reduced microglial expression of NBR1 and increased microglial expression of *miR-17* in 6-month-old 5xFAD mice but not in 2-month-old 5xFAD mice. It is possible that this delayed autophagy inhibition is a response to the gradual deposition of A β in this model after 2-months or due

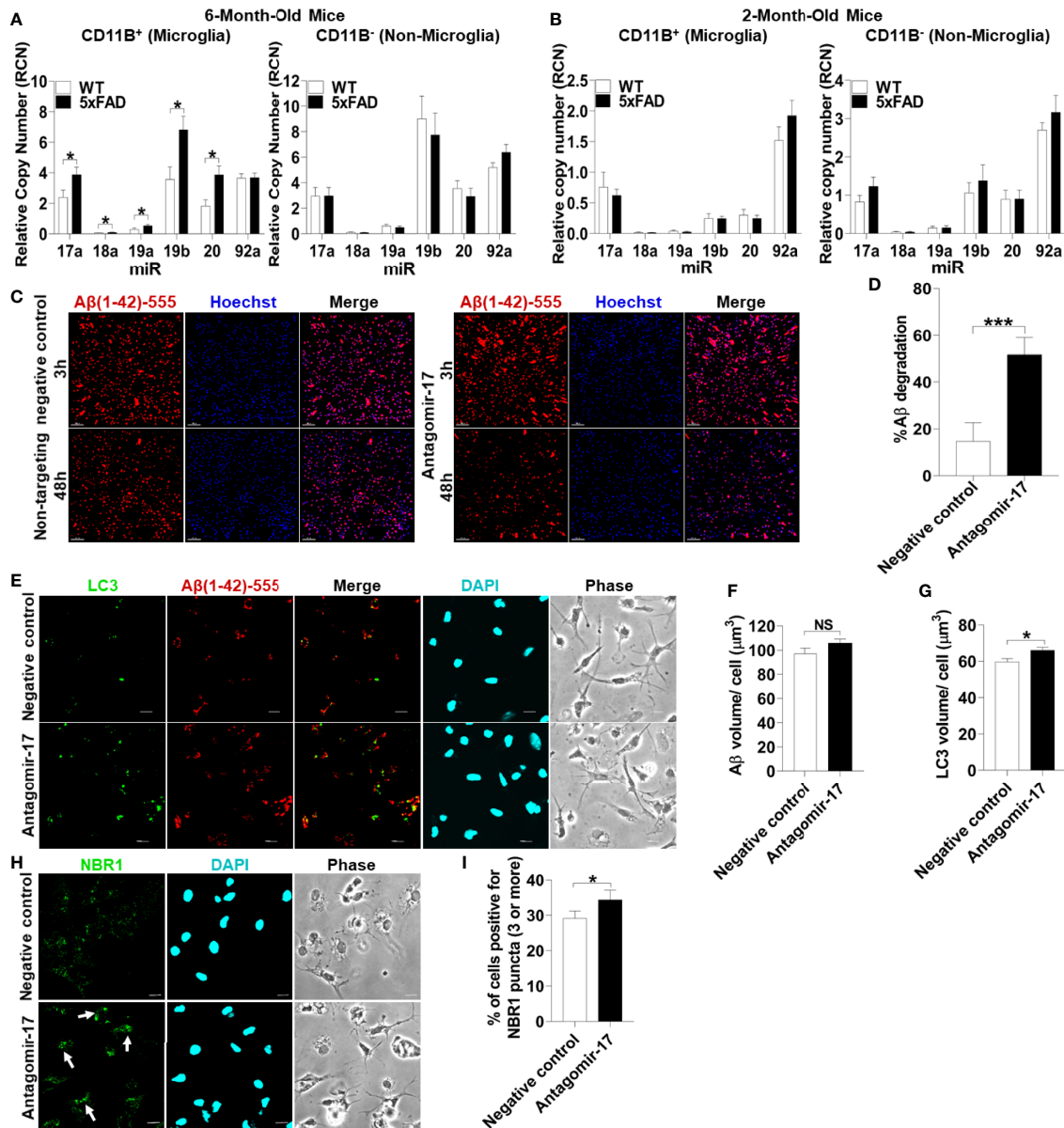


FIGURE 6 | Inhibition of upregulated *miR-17* in 5xFAD mouse microglia is sufficient to restore A β degradation, autophagy, and NBR1 puncta formation. **(A)** Relative copy number of the six miRNAs of the *Mir31/Mir-17-92* cluster in primary microglia (CD11b⁺) (left panel) and non-microglia (CD11b⁻) (right panel) fractions of 6-month-old 5xFAD and age-matched wild-type (WT) littermates' brains ($n = 12$). Statistical analysis was performed using multiple unpaired two-tailed student's t-test. **(B)** Relative copy number of the six miRNAs of the cluster in primary microglia (CD11b⁺) (left panel) and non-microglia (CD11b⁻) (right panel) fractions of 2 month old 5xFAD and age-matched wild-type (WT) littermates' brains ($n = 9$). Statistical analysis was performed using multiple unpaired two-tailed student's t-test. **(C)** Confocal images of fluorescent-A β (red) at 3 and 48h in primary microglia isolated from 5xFAD brains transfected for 48h with either antagomir-17 (50nM) or negative control inhibitor. Scale bar: 10 μ m. **(D)** Quantification of % degradation of fluorescent A β (red) by degradation assay of the images represented in **(A)** ($n = 3$). Values are % of A β volume reduction \pm SEM calculated by scoring 5 randomly chosen 20x fields of view. Statistical analysis was performed using paired two tailed Student's t-test. * $p \leq 0.05$, *** $p \leq 0.001$. **(E)** Representative confocal images of LC3 (green) in primary microglia isolated from 5xFAD brains treated with 1 μ M fluorescent-A β (red) for 2h after 48h transfection with either antagomir-17 (50nM) or negative control inhibitor. **(F)** Quantification of A β volume in the images represented in **(E)** performed using Imaris software ($n = 4$) (12 images per biologic replicate). Statistical analysis performed by paired t-test. **(G)** Quantification of LC3 volume from cells treated as in **(E)** performed using Imaris software ($n = 4$) (12 images per biologic replicate). Statistical analysis performed by paired t-test. **(H)** Representative confocal images of NBR1 (green) in primary microglia isolated from 5xFAD brains treated with 1 μ M non-fluorescent-A β for 2h after 48h transfection with either antagomir-17 (50nM) or negative control inhibitor. Arrows indicate cells with 3 or more discrete NBR1 puncta. **(I)** Quantification of the percentage of cells with 3 or more discrete NBR1 puncta from images represented in **(H)**. Quantification was performed on 10 random fields of view for each condition ($n = 3$). Statistical analysis performed by paired t-test. NS, Not Significant.

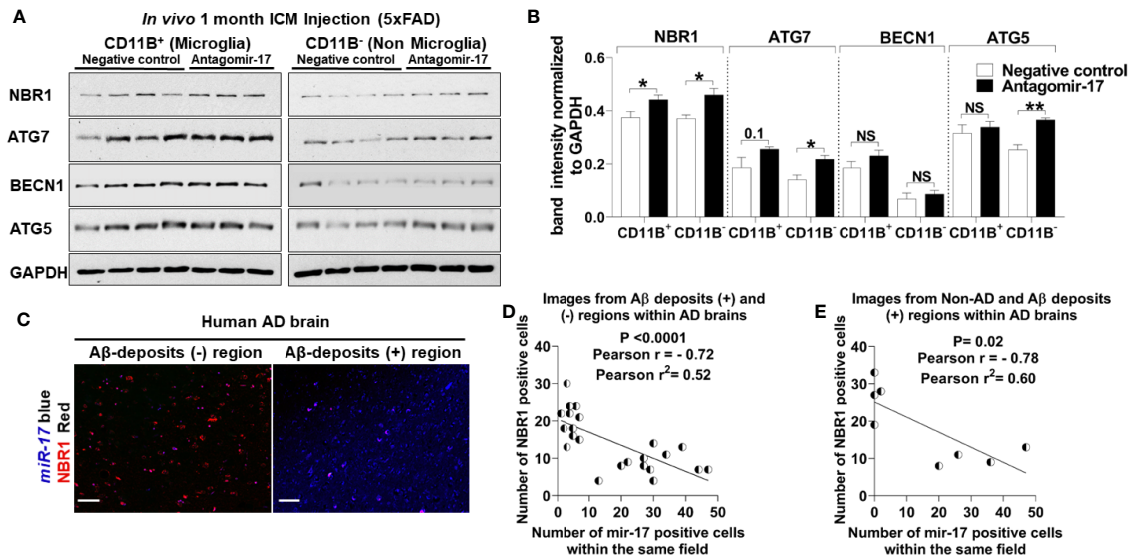


FIGURE 7 | The elevation of miR-17 expression is associated with decreased expression of NBR1 in mouse and human AD brain tissue. **(A)** NBR1, ATG7, BECN1, ATG5 and GAPDH immunoblot of primary microglia (CD11b⁺) (left panel) and non-microglia (CD11b⁻) (right panel) fractions of 2-month-old 5xFAD mice injected in their intracisterna magna (ICM) with 1.2 nmole of either antagomir-17 or non-target negative control once weekly for four weeks. **(B)** Densitometry analysis of immunoblots represented in **(A)**. Data represent mean \pm SEM (n = 4 for negative control and 3 for antagomir-17). Statistical analysis was performed using unpaired two-tailed student's t-test. **(C)** Representative images of the co-expression analysis of Immunohistochemistry of NBR1 (red) expression and *in situ* hybridization of *miR-17* (blue) in A β deposits negative (-) and positive (+) area of AD brain tissue sections. Scale bar: 100 μ M. **(D)** Pearson correlation analysis of *miR-17* and NBR1 expression in AD brains from the images represented in **(C)** (n = 4) (6 wide 20x field images are taken per replicate in which 3 images are taken from A β deposits negative and 3 images from A β deposits positive). **(E)** Pearson correlation analysis of *miR-17* and NBR1 expression in human brains (n = 8, 4 AD with A β deposits and 4 age matched no disease control) (1 wide 20x field image are taken per n). *p \leq 0.05, **p \leq 0.01, NS, Not Significant.

to other consequences downstream of A β deposition and AD pathobiology progression. On the other hand, it is possible that other factors gradually augment the expression of *miR-17* in microglia which in turn perturbs autophagy and leads to the accumulation of A β . Previous analyses of *MiR* expression in AD whole brain homogenates have not detected the upregulation of members of the cluster (51, 52). Our approach demonstrates that the expression of *miR-17* is specific to brain region, A β pathology and cell type, which may account for our discovery. Thus, it necessary to analyze individual cells instead of total homogenates where such findings may be missed.

Cargo that is destined for autophagy is selected for degradation after recognition by specific receptors, such as SQSTM1/p62, Optineurin or NBR1. Cho and colleagues demonstrated that Optineurin interacts with A β and is required for its degradation (12). However, Optineurin and p62 are highly expressed in the AD brain (12). In contrast, we demonstrate that the expression of NBR1 is decreased in human AD microglia present adjacent to A β deposits and is inversely correlated with expression of *miR-17*. The absence of NBR1 in AD microglia can explain the reduced degradation of A β . This is corroborated by the fact that in HMC3 microglia treated with siRNA to NBR1, A β degradation is significantly reduced. Importantly, p62 and Optineurin, despite their abundance in AD brains, did not substitute NBR1 and mediate A β degradation. It has been proposed that these receptors have redundant functions, however emerging reports in different

fields demonstrate that it is not always the case (14). Hence, an approach that will increase the expression of other downstream autophagy effectors without correcting NBR1 would fail to improve A β degradation in AD microglia.

Notably, we do not rule out that autophagy proteins may also play a role in phagocytosis as demonstrated by other groups (46, 47). An elegant study from Heckman and colleagues characterized a non-canonical role for autophagy marker LC3 in the uptake of A β and receptor recycling (47). This study did not observe a contribution of autophagy to degradation of A β in a microglia cell line at 24 hours. This does not contradict our findings since we used primary adult microglia and we observed a significant difference in degradation of A β at 48 hours when comparing WT to 5xFAD or *Atg5*^{-/-} microglia. Our result indicates a role for autophagy during A β degradation distinct from any dysfunction in internalization. Additionally, autophagy has other critical functions in microglia and other immune cells, including regulation of inflammation (12, 18). As *miR-17* inhibits the expression of multiple autophagy proteins, it may also impact the inflammatory response of AD microglia.

The inhibition of *miR-17* improved degradation of fluorescent-A β in primary AD microglia, and hence high expression of *miR-17* inhibits degradation. This is the first report demonstrating that the expression of a *MiR* can alter degradation function in AD microglia. We and others reported that *miR-17* has multiple proposed autophagy targets, including *Atg5*, *Becn1*, *Atg7*, *Atg12*, *Atg16L1* and *Nbr1* in other cell types

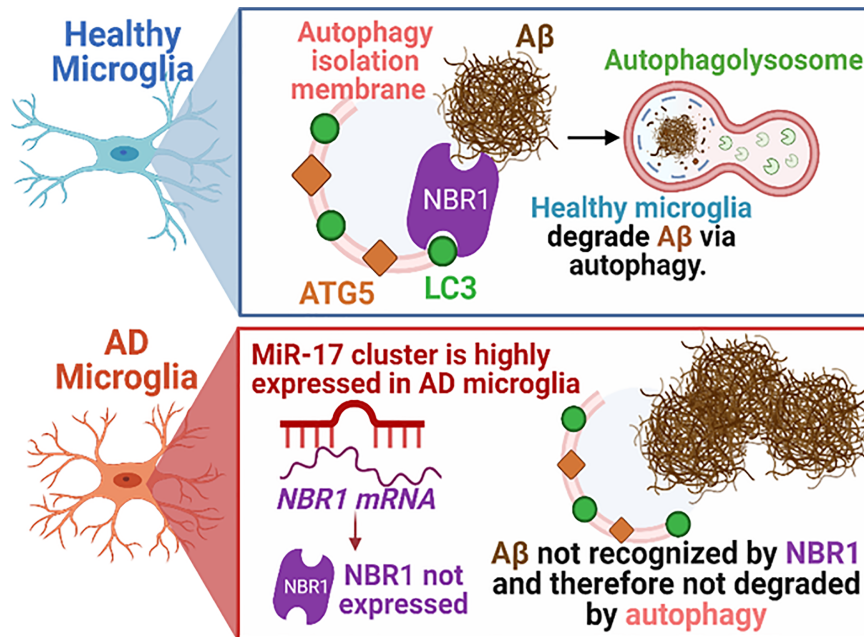


FIGURE 8 | Schematic illustration of the interplay between *miR-17*, NBR1, and A β degradation in both healthy and Alzheimer disease microglia. AD, Alzheimer's disease; ATG5, Autophagy Protein 5; NBR1, Neighbor of BRCA1 gene 1 Protein; LC3, Microtubule Associated Protein 1 Light Chain 3; A β , Amyloid beta; *miR-17*, microRNA-17. Synopsis: Autophagic clearance of A β is disrupted in primary AD mouse microglia (5xFAD). NBR1 is required for A β degradation and is downregulated in microglia in human AD in regions with high A β burden. The expression of the *Mirc1/Mir17-92* microRNA cluster is elevated in AD, including in microglia adjacent to A β plaques in human AD and in 5xFAD microglia. Elevated expression of *miR-17* correlates with reduced expression of its predicted target, autophagy receptor NBR1. Inhibiting *miR-17* in primary AD mouse microglia is sufficient to restore A β degradation, autophagy, and NBR1 puncta formation in AD microglia *in vitro* and NBR1 expression *in vivo*.

(24, 42, 43). We found that inhibition of *miR-17* improved expression of NBR1 in microglia *in vivo*, which we propose leads to improved autophagic degradation of A β . Further, we demonstrated that inhibiting *miR-17* in primary 5xFAD microglia increased expression of LC3 and accumulation of NBR1 puncta after treatment with A β . LC3 accumulation reflects increased presence of autophagosomes, indicating that reducing *miR-17* improved both A β degradation and autophagy function. NBR1 puncta are indicative of clustering of the NBR1 receptor, which can then promote continued autophagosome formation (44). These data indicate that *miR-17* is a potential therapeutic target in AD which could recover functional autophagy in microglia thus enabling improved A β clearance and improved cognition.

Several challenges may arise in seeking to measure cognition and A β clearance in 5xFAD mice. Our *in vivo* work was performed over the course of one month in a small cohort of young (2-month-old) mice. Robust differences in cognition are not observed in 5xFAD mice until about 5 months (27). Therefore, optimizing a timeline for several months of injections in a large cohort of mice will be critical. ICM injection resulted in improved expression of NBR1, ATG5 and ATG7 in non-microglial cells in our study. It is possible that inhibiting *miR-17* in all cell types may be beneficial as it could promote functional autophagy in neurons. To the best of our

knowledge, the role of NBR1 and the *Mirc1/Mir17-92* cluster in neurons in AD has not been explored warranting further mechanistic investigation. Neurons adjacent to A β -plaques express more *miR-17* and less NBR1 in human AD brain tissue. If overexpressed *miR-17* is found to be detrimental to autophagy function in neurons as well, it would be even more critical to find approaches to control *miR-17* expression as a therapeutic option in AD. Of note, this cluster of *MiRs* has many other biological functions and potential roles in AD, including that *miR-17* is shown to alter expression of the amyloid precursor protein (APP) (53). Therefore, it would be important to restore normal levels of the *MiR*, rather than completely inhibiting its expression. Alternatively, microglia-targeted therapies may be needed. This also highlights the importance of focusing on a specific *MiR* target for thorough mechanistic and therapeutic evaluation, rather than inhibiting the entire cluster. Even though other members of the *Mirc1/Mir17-92a* cluster are known to target autophagy proteins (24) and could similarly inhibit efficient A β degradation, targeting the entire cluster would also increase the number of off-target effects. Interestingly, we found increased levels of NBR1 in astrocytes in human AD. Weak autophagy activity in astrocytes expressing AD risk variant ApoE is linked to decreased clearance of A β (54). This points to the possibility that unique mechanisms of autophagy dysregulation exist within different cell types within the same region in the

same organ. As the field continues to explore therapeutic options for stimulating autophagy in AD, it will be vital to identify these unique mechanisms and ensure that we employ complementary approaches that improve autophagy function in designated cell types.

Taken together, our results indicate that autophagic clearance of A β by AD microglia is defective due to *miR-17*-mediated autophagy inhibition and reduced expression of NBR1. Improving expression of autophagy proteins by inhibiting the elevated *miR-17* improved the degradation of A β *in vitro* in microglia. Therefore, our data indicate *miR-17* is a potential therapeutic target to improve autophagic clearance of A β in AD microglia.

DATA AVAILABILITY STATEMENT

The raw data supporting the conclusions of this article will be made available by the authors, without undue reservation.

ETHICS STATEMENT

De-identified human samples were obtained in agreement with the NIH Neurobiobank or the Discovery Life Science Biobank. Written informed consent for participation was not required for this study in accordance with the national legislation and institutional requirements. The animal study was reviewed and approved by Animal Care and Use Committee (IACUC) of the Ohio State University College of Medicine.

AUTHOR CONTRIBUTIONS

Conceptualization, AA, SE, KD, and ME. Formal analysis, SE, KD, and ME. Investigation, SE, KD, ME, ND, MA, KK, AB, KH, CC, AH, AAK, HK, SN, HA, XZ, EC-B, HH, SS, AM, GN, RB, MG, and AA. Resources, AA. Writing – original draft, SE, KD, and ME. Writing – review & editing, SE, KD, ME, ND, MA, KK, AB, KH, CC, AH, AAK, HK, SN, HA, XZ, EC-B, HH, SS, AM,

GN, RB, MG, and AA. Project administration, AA, SE, KD, and ME. Supervision, AA. Funding acquisition, AA. All authors contributed to the article and approved the submitted version.

FUNDING

SE and AB were supported by funding from the Egyptian ministry of higher education. KH was supported by a Cure Cystic Fibrosis Columbus training grant and the National Institutes of Health T32 Infectious Disease Institute (OSU) training grant. KK was supported by Deutsche Forschungsgemeinschaft (DFG - German Research Foundation) and a Cystic Fibrosis Foundation Postdoctoral research grant. AA was supported by Taawon Welfare Association, West Bank, Palestine and Bank of Palestine. GN was supported by a grant from the Alzheimer's Drug Discovery Foundation (ADDF) (grant # 20160204). Studies in the Amer laboratory are supported by Ohio State University College of Medicine DFA funds and NIAID R01 AI24121 (AD supplement), NHLBI R01 HL127651-01A1, R21AG067755-01A1, R21AG064899-01A1.

ACKNOWLEDGMENTS

Images presented in this report were generated using the instruments and services at the Campus Microscopy and Imaging Facility, The Ohio State University. This facility is supported in part by grant P30 CA016058, National Cancer Institute, Bethesda, MD. The graphical abstract was created using BioRender. We would like to thank Dr. Duaa Dakhllallah for comments on the manuscript.

SUPPLEMENTARY MATERIAL

The Supplementary Material for this article can be found online at: <https://www.frontiersin.org/articles/10.3389/fimmu.2021.705581/full#supplementary-material>

REFERENCES

- Uddin MS, Stachowiak A, Al Mamun A, Tzvetkov NT, Takeda S, Atanasov AG, et al. Autophagy and Alzheimer's Disease: From Molecular Mechanisms to Therapeutic Implications. *Front Aging Neurosci* (2018) 10:4. doi: 10.3389/fnagi.2018.00004
- Lu JX, Qiang W, Yau WM, Schwieters CD, Meredith SC, Tycko R. Molecular Structure of β -Amyloid Fibrils in Alzheimer's Disease Brain Tissue. *Cell* (2013) 154:1257. doi: 10.1016/j.cell.2013.08.035
- Bateman GA, Levi CR, Schofield P, Wang Y, Lovett EC. Quantitative Measurement of Cerebral Haemodynamics in Early Vascular Dementia and Alzheimer's Disease. *J Clin Neurosci* (2006) 13:563–8. doi: 10.1016/j.jocn.2005.04.017
- Busche MA, Hyman BT. Synergy Between Amyloid- β and Tau in Alzheimer's Disease. *Nat Neurosci* (2020) 23:1183–93. doi: 10.1038/s41593-020-0687-6
- Li J-W, Zong Y, Cao X-P, Tan L, Tan L. Microglial Priming in Alzheimer's Disease. *Ann Transl Med* (2018) 6:176–6. doi: 10.21037/atm.2018.04.22
- Tamboli IY, Barth E, Christian L, Siepmann M, Kumar S, Singh S, et al. Statins Promote the Degradation of Extracellular Amyloid β -Peptide by Microglia via Stimulation of Exosome-Associated Insulin-Degrading Enzyme (IDE) Secretion. *J Biol Chem* (2010) 285:37405–14. doi: 10.1074/jbc.M110.149468
- Tajbakhsh A, Read M, Barreto GE, Ávila-Rodríguez M, Gheibi-Hayat SM, Sahebkar A. Apoptotic Neurons and Amyloid-Beta Clearance by Phagocytosis in Alzheimer's Disease: Pathological Mechanisms and Therapeutic Outlooks. *Eur J Pharmacol* (2021) 895:173873. doi: 10.1016/j.ejphar.2021.173873
- Lee CYD, Landreth GE. The Role of Microglia in Amyloid Clearance From the AD Brain. *J Neural Transm* (2010) 117:949–60. doi: 10.1007/s00702-010-0433-4
- Zuroff L, Daley D, Black KL, Koronyo-Hamaoui M. Clearance of Cerebral A β in Alzheimer's Disease: Reassessing the Role of Microglia and Monocytes. *Cell Mol Life Sci* (2017) 74:2167–201. doi: 10.1007/s00018-017-2463-7
- Hickman SE, Allison EK, El Khoury J. Microglial Dysfunction and Defective Beta-Amyloid Clearance Pathways in Aging Alzheimer's Disease Mice. *J Neurosci* (2008) 28:8354–60. doi: 10.1523/JNEUROSCI.0616-08.2008

11. Shibuya Y, Chang CCY, Huang LH, Bryleva EY, Chang TY. Inhibiting ACAT1/SOAT1 in Microglia Stimulates Autophagy-Mediated Lysosomal Proteolysis and Increases A β 1-42 Clearance. *J Neurosci* (2014) 34:14484–501. doi: 10.1523/JNEUROSCI.2567-14.2014
12. Cho MH, Cho K, Kang HJ, Jeon EY, Kim HS, Kwon HJ, et al. Autophagy in Microglia Degrades Extracellular β -Amyloid Fibrils and Regulates the NLRP3 Inflammasome. *Autophagy* (2014) 10:1761–75. doi: 10.4161/auto.29647
13. Liu R, Yang J, Liu L, Lu Z, Shi Z, Ji W, et al. An “Amyloid- β Cleaner” for the Treatment of Alzheimer's Disease by Normalizing Microglial Dysfunction. *Adv Sci* (2020) 7(2):1901555. doi: 10.1002/adv.201901555
14. Boyle KB, Randow F. The Role of “Eat-Me” Signals and Autophagy Cargo Receptors in Innate Immunity. *Curr Opin Microbiol* (2013) 16:339–48. doi: 10.1016/j.mib.2013.03.010
15. Lamark T, Kirkin V, Dikic I, Johansen T. NBR1 and P62 as Cargo Receptors for Selective Autophagy of Ubiquitinated Targets. *Cell Cycle* (2009) 8:1986–90. doi: 10.4161/cc.8.13.8892
16. Li Q, Liu Y, Sun M. Autophagy and Alzheimer's Disease. *Cell Mol Neurobiol* (2017) 37:377–88. doi: 10.1007/s10571-016-0386-8
17. Eshraghi M, Adlimoghaddam A, Mahmoodzadeh A, Sharifzad F, Yasavolisharahi H, Lorzadeh S, et al. Alzheimer's Disease Pathogenesis: Role of Autophagy and Mitophagy Focusing in Microglia. *Int J Mol Sci* (2021) 22:1–36. doi: 10.3390/ijms22073330
18. Houtman J, Freitag K, Gimber N, Schmoranzler J, Heppner FL, Jendrach M. Beclin1-Driven Autophagy Modulates the Inflammatory Response of Microglia. *via NLRP 3 EMBO J* (2019) 38(4):e99430. doi: 10.15252/embj.201899430
19. Pomilio C, Gorjod RM, Riudavets M, Vinuesa A, Presa J, Gregosa A, et al. Microglial Autophagy is Impaired by Prolonged Exposure to β -Amyloid Peptides: Evidence From Experimental Models and Alzheimer's Disease Patients. *GeroScience* (2020) 42:613–32. doi: 10.1007/s11357-020-00161-9
20. Frankel LB, Lund AH. MicroRNA Regulation of Autophagy. *Carcinogenesis* (2012) 33:2018–25. doi: 10.1093/carcin/bgs266
21. Maes O, Chertkow H, Wang E, Schipper H. MicroRNA: Implications for Alzheimer Disease and Other Human CNS Disorders. *Curr Genomics* (2009) 10:154–68. doi: 10.2174/138920209788185252
22. Hassan F, Nuovo GJ, Crawford M, Boyaka PN, Kirkby S, Nana-Sinkam SP, et al. MiR-101 and miR-144 Regulate the Expression of the CFTR Chloride Channel in the Lung. *PLoS One* (2012) 7(11):e50837. doi: 10.1371/journal.pone.0050837
23. Denk J, Boelmans K, Siegismund C, Lassner D, Arlt S, Jahn H. MicroRNA Profiling of CSF Reveals Potential Biomarkers to Detect Alzheimer's Disease. *PLoS One* (2015) 10(5):e0126423. doi: 10.1371/journal.pone.0126423
24. Tazi MF, Dakhllallah DA, Caution K, Gerber MM, Chang SW, Khalil H, et al. Elevated Mir1/Mir17-92 Cluster Expression Negatively Regulates Autophagy and CFTR (Cystic Fibrosis Transmembrane Conductance Regulator) Function in CF Macrophages. *Autophagy* (2016) 12:2026–37. doi: 10.1080/15548627.2016.1217370
25. Dellago H, Bobbili MR, Grillari J. MicroRNA-17-5p: At the Crossroads of Cancer and Aging - A Mini-Review. *Gerontology* (2016) 63:20–8. doi: 10.1159/000447773
26. Nuovo G, Paniccia B, Mezache L, Quiñónez M, Williams J, Vandiver P, et al. Diagnostic Pathology of Alzheimer's Disease From Routine Microscopy to Immunohistochemistry and Experimental Correlations. *Ann Diagn Pathol* (2017) 28:24–9. doi: 10.1016/j.aanddiagnpath.2017.02.006
27. Oakley H, Cole SL, Logan S, Maus E, Shao P, Craft J, et al. Intraneuronal β -Amyloid Aggregates, Neurodegeneration, and Neuron Loss in Transgenic Mice With Five Familial Alzheimer's Disease Mutations: Potential Factors in Amyloid Plaque Formation. *J Neurosci* (2006) 26:10129–40. doi: 10.1523/JNEUROSCI.1202-06.2006
28. Sasaguri H, Nilsson P, Hashimoto S, Nagata K, Saito T, De Strooper B, et al. APP Mouse Models for Alzheimer's Disease Preclinical Studies. *EMBO J* (2017) 36:2473–87. doi: 10.15252/embj.201797397
29. Zhao Z, Thackray LB, Miller BC, Lynn TM, Michelle M, Ward E, et al. Coronavirus Replication Does Not Require the Autophagy Gene ATG5 Zjiang. *Autophagy* (2007) 3(6):581–5. doi: 10.4161/auto.4782
30. Gage GJ, Kipke DR, Shain W. Whole Animal Perfusion Fixation for Rodents. *J Vis Exp* (2012) (65):3564. doi: 10.3791/3564
31. Alzate-Correa D, Mei-ling Liu J, Jones M, Silva TM, Alves MJ, Burke E, et al. Neonatal Apneic Phenotype in a Murine Congenital Central Hypoventilation Syndrome Model is Induced Through non-Cell Autonomous Developmental Mechanisms. *Brain Pathol* (2020) 0:1–19. doi: 10.1111/bpa.12877
32. Guneykaya D, Ivanov A, Hernandez DP, Haage V, Wojtas B, Meyer N, et al. Transcriptional and Translational Differences of Microglia From Male and Female Brains. *Cell Rep* (2018) 24:2773–83. doi: 10.1016/j.celrep.2018.08.001
33. Zöller T, Schneider A, Kleimeyer C, Masuda T, Potru PS, Pfeifer D, et al. Silencing of Tgfb Signalling in Microglia Results in Impaired Homeostasis. *Nat Commun* (2018) 9:1–13. doi: 10.1038/s41467-018-06224-y
34. Lorenzo A, Yankner BA. Beta-Amyloid Neurotoxicity Requires Fibril Formation and is Inhibited by Congo Red. *Proc Natl Acad Sci* (1994) 91:12243–7. doi: 10.1073/pnas.91.25.12243
35. Bordt EA, Block CL, Petrozziello T, Sadri-Vakili G, Smith CJ, Edlow AG, et al. Isolation of Microglia From Mouse or Human Tissue. *STAR Protoc* (2020) 1:100035. doi: 10.1016/j.xpro.2020.100035
36. Klionsky DJ, Abdelmohsen K, Abe A, Abedin J, Abeliovich H, Bartolom A, et al. Guidelines for the Use and Interpretation of Assays for Monitoring Autophagy (3rd Edition). *Autophagy* (2016) 12(1):1–222. doi: 10.1080/15548627.2015.1100356
37. Gavrilin MA, Bouakl IJ, Knatz NL, Duncan MD, Hall MW, Gunn JS, et al. Internalization and Phagosome Escape Required for Francisella to Induce Human Monocyte IL-1 β Processing and Release. *Proc Natl Acad Sci USA* (2006) 103:141–6. doi: 10.1073/pnas.0504271103
38. Sobesky JL, Barrientos RM, May HS De, Thompson BM, Weber D, Watkins LR, et al. High-Fat Diet Consumption Disrupts Memory and Primes Elevations in Hippocampal IL-1 β , an Effect That can be Prevented With Dietary Reversal or IL-1 Receptor Antagonism. *Brain Behav Immun* (2014) 42:22–32. doi: 10.1016/j.bbi.2014.06.017
39. Barrientos RM, Hein AM, Frank MG, Watkins LR, Maier SF. Intracisternal Interleukin-1 Receptor Antagonist Prevents Postoperative Cognitive Decline and Neuro Inflammatory Response in Aged Rats. *J Neurosci* (2012) 32:14641–8. doi: 10.1523/JNEUROSCI.2173-12.2012
40. Bohlen CJ, Bennett FC, Bennett ML. Isolation and Culture of Microglia. *Curr Protoc Immunol* (2019) 125:e70. doi: 10.1002/cpim.70
41. Yamamoto M, Horiba M, Buescher JL, Huang D, Gendelman HE, Ransohoff RM, et al. Overexpression of Monocyte Chemotactic Protein-1/CCL2 in β -Amyloid Precursor Protein Transgenic Mice Show Accelerated Diffuse β -Amyloid Deposition. *Am J Pathol* (2005) 166:1475–85. doi: 10.1016/S0002-9440(10)62364-4
42. Karagkouni D, Paraskevopoulou MD, Chatzopoulos S, Vlachos S, Tastsoglou S, Kanellos I, et al. DIANA-TarBase V8: A Decade-Long Collection of Experimentally Supported miRNA – Gene Interactions. *Nucleic Acids Res* (2018) 46:239–45. doi: 10.1093/nar/gkx1141
43. Grosswendt S, Filipchuk A, Manzano M, Klironomos F, Herzog M, Gottwein E, et al. Unambiguous Identification of miRNA:Target Site Interactions by Different Types of Ligation Reactions. *Mol Cell* (2014) 54:1042–54. doi: 10.1016/j.molcel.2014.03.049.Unambiguous
44. Ohnstad AE, Delgado JM, North BJ, Nasa I, Kettenbach AN, Schultz SW, et al. Receptor-Mediated Clustering of FIP200 Bypasses the Role of LC3 Lipidation in Autophagy. *EMBO J* (2020) 39:1–20. doi: 10.15252/embj.2020104948
45. Klionsky DJ, Abdel-Aziz AK, Abdelfatah S, Abdellatif M, Abdoli A, Abel S, et al. Guidelines for the Use and Interpretation of Assays for Monitoring Autophagy (4th Edition). *Autophagy* (2021) 17(1):1–382. doi: 10.1080/15548627.2020.1797280
46. Lucin KM, O'Brien CE, Bieri G, Czirr E, Mosher KI, Abbey RJ, et al. Microglial Beclin 1 Regulates Retromer Trafficking and Phagocytosis and Is Impaired in Alzheimer's Disease. *Neuron* (2013) 79(5):873–86. doi: 10.1016/j.neuron.2013.06.046
47. Heckmann BL, Teubner BJW, Tummers B, Guy CS, Zakharenko SS, Green DR. LC3-Associated Endocytosis Facilitates β -Amyloid Clearance and Mitigates Neurodegeneration in Murine Alzheimer's Disease. *Cell* (2019) 178:536–51. doi: 10.1016/j.cell.2019.05.056
48. Comincini S, Allavena G, Palumbo S, Morini M, Durando F, Angeletti F, et al. MicroRNA-17 Regulates the Expression of ATG7 and Modulates the Autophagy Process, Improving the Sensitivity to Temozolomide and Low-Dose Ionizing Radiation Treatments in Human Glioblastoma Cells. *Cancer Biol Ther* (2013) 14:574–86. doi: 10.4161/cbt.24597
49. Maday S. Mechanisms of Neuronal Homeostasis: Autophagy in the Axon. *Brain Res* (2016) 1649:143–50. doi: 10.1016/j.brainres.2016.03.047
50. Krause K, Kopp BT, Tazi MF, Caution K, Hamilton K, Badr A, et al. The Expression of Mir1/Mir17-92 Cluster in Sputum Samples Correlates With

- Pulmonary Exacerbations in Cystic Fibrosis Patients. *J Cyst Fibros* (2018) 17:454–61. doi: 10.1016/j.jcf.2017.11.005
51. Lukiw WJ. Micro-RNA Speciation in Fetal, Adult and Alzheimer's Disease Hippocampus. *Neuroreport* (2007) 18:297–300. doi: 10.1097/WNR.0b013e3280148e8b
52. Rahman MR, Islam T, Zaman T, Shahjaman M, Karim MR, Huq F, et al. Identification of Molecular Signatures and Pathways to Identify Novel Therapeutic Targets in Alzheimer's Disease: Insights From a Systems Biomedicine Perspective. *Genomics* (2020) 112:1290–9. doi: 10.1016/j.ygeno.2019.07.018
53. Delay C, Calon F, Mathews P, Hébert SS. Alzheimer-Specific Variants in the 3'UTR of Amyloid Precursor Protein Affect microRNA Function. *Mol Neurodegener* (2011) 6:70. doi: 10.1186/1750-1326-6-70
54. Simonovitch S, Schmukler E, Bepalko A, Iram T, Frenkel D, Holtzman DM, et al. Impaired Autophagy in APOE4 Astrocytes. *J Alzheimer's Dis* (2016) 51:915–27. doi: 10.3233/JAD-151101

Conflict of Interest: AM and GN were employed by Gnome Diagnostic.

The remaining authors declare that the research was conducted in the absence of any commercial or financial relationships that could be construed as a potential conflict of interest.

Publisher's Note: All claims expressed in this article are solely those of the authors and do not necessarily represent those of their affiliated organizations, or those of the publisher, the editors and the reviewers. Any product that may be evaluated in this article, or claim that may be made by its manufacturer, is not guaranteed or endorsed by the publisher.

Copyright © 2021 Estfanous, Daily, Eltobgy, Deems, Anne, Krause, Badr, Hamilton, Carafice, Hegazi, Abu Khweek, Kelani, Nimjee, Awad, Zhang, Cormet-Boyaka, Haffez, Soror, Mikhail, Nuovo, Barrientos, Gavrilin and Amer. This is an open-access article distributed under the terms of the Creative Commons Attribution License (CC BY). The use, distribution or reproduction in other forums is permitted, provided the original author(s) and the copyright owner(s) are credited and that the original publication in this journal is cited, in accordance with accepted academic practice. No use, distribution or reproduction is permitted which does not comply with these terms.